Unbinned Likelihood Analysis for X-ray Polarization

Denis González-Caniulef★[1], Ilaria Caiazzo†[2], Jeremy Heyl‡[1]
[1]Department of Physics and Astronomy, University of British Columbia, Vancouver, BC V6T 1Z1, Canada
[2]TAPIR, Walter Burke Institute for Theoretical Physics, Mail Code 350-17, Caltech, Pasadena, CA 91125, USA

Accepted XXX. Received YYY; in original form ZZZ

ABSTRACT

We present a systematic study of the unbinned likelihood technique, which can be used as an alternative method to analyse phase-dependent, X-ray spectro-polarimetric observations obtained with IXPE and other photo-electric polarimeters. We apply the unbinned technique to models of the luminous X-ray pulsar Hercules X-1, for which we produce simulated observations using IXPEObsSim package. We consider minimal knowledge about the actual physical process responsible for the polarized emission from the accreting pulsar and assume that the observed phase-dependent polarization angle can be described by the rotating vector model. Using the unbinned technique, the detector's modulation factor, and the polarization information alone, we found that both the rotating vector model and the underlying spectro-polarimetry model can reconstruct equally well the geometric configuration angles of the accreting pulsar. However, the measured polarization fraction becomes biased with respect to underlying model unless the energy redistribution and effective area of the detector are also taken into account. For the different analyses, we obtain posterior distributions from multiple IXPEObsSim realizations and show that the unbinned technique yields $\sim 10\%$ smaller error bars than the binned technique. We also discuss alternative sources, such as magnetars, in which the unbinned technique and the rotating vector model might be applied.

Key words: techniques: polarimetric — X-rays: general — methods: data analysis — methods: statistical —

1 INTRODUCTION

The Imaging X-ray Polarimetry Explorer mission (IXPE, Weisskopf et al. 2016) was successfully launched on December 2021, opening a new window to study X-ray sources and physical processes in extreme astrophysical environments. IXPE consists of three identical telescopes, each of them carrying an independent Gas Pixel Detector (GPD) polarimeter instrument ($2-8$ keV range), whose technology is based on the photoelectric effect (Costa et al. 2001; Bellazzini et al. 2007). A beam of radiation from a source results in multiple photoelectron tracks in the GPD, from which is possible to reconstruct the initial energy and polarization direction of single photons. The rich polarimetric information contained in IXPE observations naturally push the development of new data analysis techniques.

The analysis of X-ray observations often rely on the binning technique, in which a list of photons is pre-processed by grouping them into bins (e.g. in energy bins, phase bins, etc.) and then characterized by the counts in each interval. Inevitably, information is lost by binning the events. This loss can be mitigated by a large sampling of the data or by adapting the binning according the different science cases, which usually do not have a unique criteria. However, this becomes a major issue when the analysis has to deal with scarce data, e.g. low count rates, large background component, etc.

An alternative method to the binned analysis is the photon-by-photon likelihood analysis, also know as unbinned likelihood method. This method has been already routinely used, for example in gamma-ray astronomy, and it has been also discussed for X-ray polarimetry (see e.g. Marshall 2021), as well as in the context of photoelectron track analysis (using convolutional neural networks), aiming to improve the sensitivity (modulation factor) of GPDs (Peirson et al. 2021; Peirson & Romani 2021). Our goal is to use the unbinned technique to compare a model against photon-by-photon events, to achieve a higher sensitivity beyond the chi-square analysis of binned X-ray polarimetry data (see e.g. Kislat et al. 2015). Besides extracting the maximum amount of information from the data, the unbinned technique can be implemented quite economically even when a variety of instrumental response functions need to be considered in the analysis.

We study the unbinned technique and apply it to simulations of IXPE observations of the accreting X-ray pulsar Hercules X-1 (hereafter Her X-1), which is one of the main targets in IXPE's long term plan. The simulations are generated using IXPEObsSim package (Pesce-Rollins et al. 2019), while the model for the polarized X-ray emission from the X-ray pulsar is taken from Caiazzo & Heyl (2021a) and Caiazzo & Heyl (2021b). We perform various tests for the binned and unbinned technique, comparing the simulated data with the rotating vector model (RVM) and the underlying model. We also include the detector energy dispersion in the unbinned technique and present an example to implement it in Python.

The paper is organized as follows. In § 2, we present the method and derivation of the unbinned technique. In § 3, we discuss the results of our analysis of Her X-1 simulated data using the unbinned and binned technique. Conclusions are presented in § 4.

★ dgonzalez@phas.ubc.ca; CITA National Fellow
† email: ilariac@caltech.edu; Sherman Fairchild Fellow
‡ email: heyl@phas.ubca.ca

2 THE METHOD

The IXPE observatory consists of three X-ray telescopes mounted in parallel, each feeding radiation into a gas-pixel detector. The X-ray photons are absorbed by atoms in the gas (dimethyl ether) and ionize an electron from the K-shell. The ionization is typically well above the threshold of the particular atom, so the cross section decreases with increasing photon energy. Furthermore, the outgoing electron is approximately in a well-defined momentum state; the direction of the momentum correlates with the photon electric field with a $\cos^2\psi$ dependence.

The magnitude of the correlation for fully linearly polarized radiation is known as the modulation factor. By modelling the high-energy photo-electron track (Sgrò 2017), the following properties of the incoming photon can be determined: energy, arrival time, electron direction and position on the sky. As the energy of the photon increases, so does the momentum of the photo-electron, which results in a longer and more easily measured track, and therefore the modulation factor for IXPE increases with increasing energy from 15% at 2 keV to 60% at 8 keV (Weisskopf et al. 2021).

We can build the likelihood function focusing only on the polarization signal, which is a function of photon angle, energy and time, or by including the spectrum, which is just a function of energy and time, in the model as well (see also Kislat et al. 2015; Marshall 2021). Let $p_0(E,t)$ be polarization degree of the model, $\mu(E)$ be the modulation factor of the instrument and $\psi_0(E,t)$ be the polarization angle of the model; the first component of the likelihood function can therefore be written as:

$$f(\psi) = \frac{1}{2\pi}\left[1 + \mu p_0\left(2\cos^2(\psi-\psi_0) - 1\right)\right]$$

where ψ is the angle of a particular photon and the energy and time variables are suppressed. This expression results from the definition of the modulation factor, the differential scattering cross-section, and the normalization $\int f(\psi)d\psi = 1$, which is constant with respect to the expected degree of polarization. We can reformulate it as

$$f(\psi) = \frac{1}{2\pi}\left[1 + \mu p_0\left[\cos 2\psi\cos 2\psi_0 + \sin 2\psi \sin 2\psi_0\right]\right],$$

and, if we define $Q_m = p_0\cos 2\psi_0$ and $U_m = p_0 \sin 2\psi_0$ for the model, and $Q_\gamma = \cos 2\psi$ and $U_\gamma = \sin 2\psi$ for the photon, we have

$$f(\psi) = \frac{1}{2\pi}\left[1 + \mu\left[Q_\gamma Q_m + U_\gamma U_m\right]\right]$$

If we want to include the spectrum ($I(E,t)$) in the model as well, we can write

$$f_i = \frac{1}{2\pi}\left[1 + \left(\mu\left[Q_\gamma Q_m + U_\gamma U_m\right]\right)\right] I = \frac{1}{2\pi}\mathbf{S}_\gamma M \mathbf{S}$$

where $\mathbf{S}$ are the Stokes parameters predicted by the model for the energy and arrival time of the photon, $\mathbf{S}_\gamma$ are the Stokes parameters of the detected photon and M is the modulation matrix for the energy of the photon. M is a property of the instrument; for IXPE it can be written as

$$M = \begin{bmatrix} 1 & 0 & 0 & 0 \\ 0 & \mu(E) & 0 & 0 \\ 0 & 0 & \mu(E) & 0 \\ 0 & 0 & 0 & 0 \end{bmatrix},$$

where $\mu(E)$ is the modulation factor as a function of energy. The last diagonal term is zero because IXPE does not detect circular polarization. The matrix can have off-diagonal terms if there is mixing between polarization states (in the second to last columns) or if the instrument exhibits spurious polarization (in the first column). In the case of IXPE, the effects of spurious polarization are accounted for by adding a term to the values of Q_γ and U_γ.

The photon polarization vector is

$$\mathbf{S}_\gamma = \begin{bmatrix} 1 \\ \cos 2\psi \cos 2\chi \\ \sin 2\psi \cos 2\chi \\ \sin 2\chi \end{bmatrix}.$$

For IXPE, $\chi = 0$ as the instrument does not detect circular polarization. The total logarithmic likelihood of the data given the model is

$$\log L = \sum \log f_i - N_{\rm pred},$$

where $N_{\rm pred}$ is the number of photons predicted by the model. For the more general situation where the instrument is also capable of detecting circular polarization we have

$$M = \begin{bmatrix} 1 & 0 & 0 & 0 \\ 0 & \mu(E) & 0 & 0 \\ 0 & 0 & \mu(E) & 0 \\ 0 & 0 & 0 & \mu(E) \end{bmatrix}$$

assuming that the three modulation factors are equal.

3 RESULTS

As a first check, we simulate 1,000 fully polarized photons ($Q/I = \frac{1}{2}\sqrt{2}$ and $U/I = \frac{1}{2}\sqrt{2}$) assuming a modulation factor of unity and we recover the value of Q/I and U/I using both the unbinned likelihood estimator and the Kislat et al. (2015) binned estimator, twice the weighted (inversely with modulation factor) mean of Q_γ and U_γ. We find that both estimators are unbiased and the unbinned estimator is about 32% more efficient than the Kislat et al. (2015) estimator. The standard deviation of Q/I and U/I over 100,000 realisations is 2.93% versus 3.86%. The latter value is agrees with the Kislat et al. (2015) estimate of the variance. The increased efficiency means that for fully polarized radiation one can achieve the same precision with a 40% shorter exposure time. For unpolarized radiation, the two techniques perform equally well with a standard deviation of 4.4% following the Kislat et al. (2015) formula. Although the unbinned technique is more efficient for polarized sources, the key advantages come into play when one expects the polarization to vary with time according to an underlying model and more subtly when the polarization varies with energy.

3.1 IXPEObsSim simulation

We test the unbinned technique using the models for X-ray emission from X-ray pulsars from Caiazzo & Heyl (2021a) and Caiazzo & Heyl (2021b) by varying the geometric parameters of the pulsar.

The pulsar model is tabulated in a file containing the spectra and Stokes parameters for 10^3 energy bins logarithmically spaced between 0.5 to 77.9 keV, and a mesh of 10^5 line-of-sight angles relative to the magnetic axis. Since the Stokes parameters for the tabulated models are defined relative to the direction of the magnetic field axis of the pulsar, which is also axisymmetric, only Q/I is relevant, while $U/I = 0$ in that frame. The model is generalized to account for the pulsar rotation considering an arbitrary line-of-sight angle α and magnetic axis angle β with respect to the spin axis, with the Stokes Q and U redefined relative to the spin axis as well (see Appendix C in Caiazzo & Heyl 2021a). The model spectrum is normalized according to the spectral flux from *NuSTAR* observations

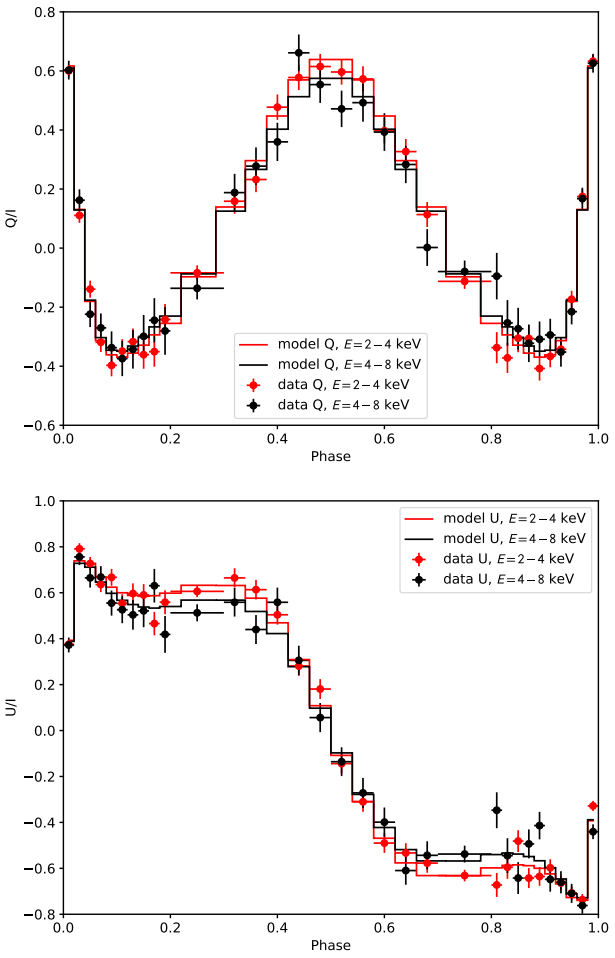

Figure 1. Phase-dependent Stokes parameters for for Her X-1. The point with error bars correspond to 100 ks simulation with IXPEObsSim. The solid lines correspond to the binned underlying model of (Caiazzo & Heyl 2021b)

(Wolff et al. 2016), considering a neutral hydrogen column density $N_{\rm H} = 1.7 \times 10^{20}$ cm^{-2} (Fürst et al. 2013).

We generate periodic point source simulations of Her X-1 using IXPEObsSim package (version 18.0.0). In the following all simulations are run for 100-ks *IXPE* observations. No background or spurious modulation are included in the simulations. For all simulations, we set the pulsar angles $\alpha = 52°$ and $\beta = 42°$. For the pulsar ephemeris, we account only for the rotational frequency of the pulsar $f_0 = 0.806$ Hz, while other parameters such as the frequency derivative and orbital period of the binary, for simplicity, are ignored.

We generate a photon list stored in FITS files computed from the main Monte Carlo simulation, accounting for the instrument response functions of each IXPE detector. The events are phase-folded and further selected in in 2−8 keV range. Finally, the events are binned considering 2 energy bins with (2−4 and 4−8 keV) and thirty phase bins with ten evenly spaced in phase from 0.3 to 0.7 and thirty from 0.8 to 0.2. Figure 1 shows the resulting simulated Stokes Q/I and U/I data for a single IXPEObsSim realization, as well as the underlying model.

3.2 Binned vs Unbinned analysis: No energy dispersion

We first perform the polarimetry analysis confronting the simulated data with the models, taking into account only the detector's modulation factor. The analysis including the detector's energy dispersion is discussed in Section 3.3.

3.2.1 Rotating vector model

The accretion process coupled with transport of polarized radiation in a strongly magnetized NS is highly non-trivial. Therefore, we first analyse the data in the scenario that the underlying physical mechanism for the polarized emission from Her X-1 is unknown. However, we assume that the accretion is funneled into the magnetic poles through an axisymmetric magnetic field and that the radiation is emitted in the X-mode or O-mode. Then, as a first approximation, the polarization angle of the radiation is determined by the direction of the pulsar magnetic axis relative to the spin axis, which can be modeled using the RVM (Radhakrishnan & Cooke 1969). The main idea is to reconstruct the geometric configuration of the pulsar using the information contained only in the phase-dependent polarization angle, leaving the polarization degree and spectral flux un-modelled.

Similarly, the RVM might be also applied to other magnetized sources such as magnetars. As predicted by QED, under strong magnetic fields the vacuum becomes birefringent. This means that the radiation propagates in the magnetar's magnetosphere readapting the X- and O-mode to the local magnetic field. The main effect for a magnetar is that the polarization angle detected by a distant observer reflects the magnetic field direction far from the NS's surface, where the field across the plane perpendicular to the line-of-sight is nearly uniform (Heyl & Shaviv 2000, 2002). If the topology of the magnetic field is dominated by a dipolar component, without a strong toroidal component (or twist), then the polarization angle is determined by the direction of magnetic axis with respect to the spin axis. In this context, the RVM can be applied to analyse the phase-dependent polarization angle in the lower energy range of the soft X-ray spectrum, where X-ray photons have a low optical depth to resonant cyclotron scattering by charged particles streaming in the magnetar's magnetosphere.

We compare the RVM to simulated IXPE data for Her X-1 using both binned and unbinned analyses (in the 2 – 4 keV range). We first test the methods with a single IXPEObsSim realization. We fit the RVM to the polarization angle considering four free parameters: α and β angles, a rotation in the position angle in the sky and a deviation from the initial phase. Additionally, for the unbinned analysis, we allow the likelihood function to measure the mean polarization degree of the source, leaving p_0 as a free parameter that can be adjust to the data. Fig 2 shows the best fitted RVM curves and Figure 3 shows the associated error parameters obtained with the binned and unbinned analysis. We found that using the RVM alone is possible to reconstruct the geometric angles of the pulsar. As shown in Fig 3, the α and β solutions obtained with the unbinned technique are well centered around the actual angles of the pulsar. The binned analysis return α and β solutions that are slightly biased, a bit more than 1σ with respect to the actual angles of the input model. We also found that the error parameters obtained with the unbinned technique are smaller than the binned technique. For the single IXPEObsSim realization, the errors from the binned technique are approximately $(\sigma_{\rm bin} - \sigma_{\rm ubin})/\sigma_{\rm ubin} \sim 30\%$ larger than those obtained with the unbinned technique.

Due to the stochastic component of the IXPEObsSim simulations, different realizations produce different parameter estimations. In or-

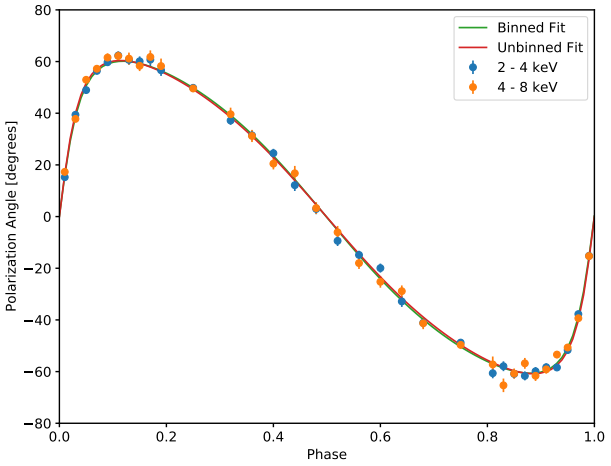

Figure 2. The measured polarization angle from a simulated 100-ks observations of Her X-1 using the model of Caiazzo & Heyl (2021b). The results of a fit to the binned data from 2−4 keV and an unbinned fit to the photons identified with energies from 2−4 keV.

der to further investigate the error estimations and potential bias discussed above, we run multiple IXPEObsSim realizations. Fig. 4 shows the posterior distribution for the best fitted parameters obtained with $\sim 12,000$ realizations, applying simultaneously the binned and unbinned technique. We found that the binned technique produces error estimations $(\sigma_{\rm bin} - \sigma_{\rm ubin})/\sigma_{\rm ubin} \sim 10\%$ larger than the binned technique (which is smaller than the 30% difference found with the single realization). More remarkably, the unbinned technique produces unbiased parameter estimations (except for the mean polarization degree, which is discussed in Sec. 3.2.2 and 3.3), while the binned technique produces slightly biased estimations, confirming what we observed with the single realization. In particular, for the α and β angles, we found that the bias present in the binned technique is not dramatic and still within the 1σ error estimation.

3.2.2 *Underlying model*

As in previous section, we repeat the polarimetry analysis, but now comparing the simulated data against the underlying model (Caiazzo & Heyl 2021b). We proceed with the analysis of multiple IXPEObsSim realization as follows:

- We consider five free parameters for fitting the model to the data: the α and β angles, a rotation of the position angle on the sky, a fractional deviation for the polarization degree with respect to the model and the initial phase when the magnetic axis crosses the meridian of the line of sight.
- In the unbinned technique, we account only for the detector modulation factor in the likelihood function.
- For the binned technique, the model is binned in phase and energy in the Stokes parameter space, without extra considerations. The best parameter estimation is obtained by minimizing the chi-square between data and model, accounting for the covariance between U/I and Q/I as explained in Kislat et al. (2015).
- The simulated data for the Stokes Q and U are binned in phase and energy as discussed earlier.

Fig. 5 shows the posterior distribution for the best fitted parameters obtained simultaneously with the binned and unbinned technique. We confirm the $\sim$ 10% larger error estimation of the binned technique with respect to those obtained with the unbinned analysis (consistent with the analysis in Sec. 3.2.1). More remarkably, we found a significant bias in the measured polarization degree, more than 1σ away from the central value of the underlying model (also consistent with the analysis in Sec. 3.2.1). That effect is present in both the binned and unbinned analysis, but it is stronger in the latter. These results show that in order to obtain precise measurement of the polarization degree of a source, the analysis needs to account for additional instrumental response functions beside the modulation factor, which is discussed in the next section.

3.3 Unbinned analysis including energy dispersion

The IXPEObsSim package provides additional instrument response functions besides the modulation factor, such as the energy dispersion, effective area, point spread function, and vignetting of each detector unit. We further refine the unbinned analysis presented in the previous section by convolving the underlying model with the energy dispersion and effective area, in addition to the modulation factor. The vignetting is not considered in the analysis as it is relevant only for extended sources.

More concretely, we calculate the following convolved Stokes models for detector units $u = 1, 2, 3$:

$$\langle \mu_u Q_m \rangle = \frac{\int A_u(E) R_u(E, E') C_m(E, \phi) \mu_u(E) Q_m(E, \phi) \mathrm{d}E}{\int A_u(E) R_u(E, E') C_m(E, \phi) \mathrm{d}E}$$

$$\langle \mu_u U_m \rangle = \frac{\int A_u(E) R_u(E, E') C_m(E, \phi) \mu_u(E) U_m(E, \phi) \mathrm{d}E}{\int A_u(E) R_u(E, E') C_m(E, \phi) \mathrm{d}E}$$

where A_u is the effective area, R_u is the energy dispersion, $C_m = I_m/E$ is the model count spectrum, E' is the detector channel, and ϕ and E correspond to the model phase and energy, respectively. The convolved models $\langle \mu_u Q_m \rangle$ and $\langle \mu_u U_m \rangle$ are phase-dependent, channel-dependent, and detector-unit-dependent. In analogy to the estimator f_i presented in Sec 2, we re-define a new estimator to analyse just the polarization information of the source:

$$f = \frac{1}{2\pi} \left[1 + \langle \mu_u Q_m \rangle Q_\gamma + \langle \mu_u U_m \rangle U_\gamma \right],$$

which can be used to calculate a energy-dispersed likelihood function. However, with this new estimator we are not longer able to analyze the polarization information completely alone (as in in Sec 2) as it gets mixed with the source spectrum in the convolved models.

We repeat the analysis presented in § 3.2.2 including now the energy dispersion (see sample code in Appendix A). Fig. 6 shows the posterior distribution for the best fitted parameters obtained with multiple IXPEObsSim realizations. They all remain unchanged for the three parameters α, β, and position angle. However, for the fractional deviation of the polarization degree, the error bars are now centered around zero, removing the bias observed in Fig. 5. The polarization degree of the underlying model can be reconstructed with actual precision better than 1%. The inclusion of the energy dispersion reduce the bias by a factor of about 24..

4 CONCLUSIONS

We presented a systematic study of the unbinned likelihood technique. We applied it to simulated IXPE observations of Her X-1, using IXPEObsSim package and the model of Caiazzo & Heyl (2021b). As a first test, we assume minimal knowledge about the physical

mechanism responsible for the X-ray polarized emission and analyze the simulated data using the RVM.

We found that the RVM can reconstruct the geometric configuration of Her X-1 using just the phase-dependent polarization angle and the detector modulation factor. By generating posterior distributions from multiple IXPEObsSim realizations, we found the unbinned technique and the RVM return unbiased configuration angles. Instead, the binned technique and the RVM return slightly biased configuration angles.

On the other hand, using the underlying model and the modulation factor, we found that both the binned and unbinned technique return a substantial biased polarization degree relative to the model. Instead, the configuration angles can be reconstructed in a unbias manner with the unbinned technique, but again they are slightly bias for the binned technique.

If we account for the energy dispersion of the detector, then the unbinned technique returns an unbiased estimate of the polarization degree. We also show explicitly that the unbinned technique, including the energy dispersion, can be implemented economically, transparently, and in a straightforward manner in `Python`.

ACKNOWLEDGEMENTS

This work was supported by the Natural Sciences and Engineering Research Council of Canada (NSERC), [funding reference #CITA 490888-16]. IC is a Sherman Fairchild Fellow at Caltech and thanks the Burke Institute at Caltech for supporting her research. This research was enabled in part by support provided by WestGrid (www.westgrid.ca) and Compute Canada (www.computecanada.ca). This research makes use of the SciServer science platform (www.sciserver.org).

DATA AVAILABILITY

Upon request, the corresponding author will provide the software to reproduce the simulations performed in this work.

REFERENCES

Bellazzini R., et al., 2007, Nuclear Instruments and Methods in Physics Research A, 579, 853
Caiazzo I., Heyl J., 2021a, MNRAS, 501, 109
Caiazzo I., Heyl J., 2021b, MNRAS, 501, 129
Costa E., Soffitta P., Bellazzini R., Brez A., Lumb N., Spandre G., 2001, Nature, 411, 662
Fürst F., et al., 2013, ApJ, 779, 69
Heyl J. S., Shaviv N. J., 2000, MNRAS, 311, 555
Heyl J. S., Shaviv N. J., 2002, Phys. Rev. D, 66, 023002
Kislat F., Clark B., Beilicke M., Krawczynski H., 2015, Astroparticle Physics, 68, 45
Marshall H. L., 2021, AJ, 162, 134
Peirson A. L., Romani R. W., 2021, ApJ, 920, 40
Peirson A. L., Romani R. W., Marshall H. L., Steiner J. F., Baldini L., 2021, Nuclear Instruments and Methods in Physics Research A, 986, 164740
Pesce-Rollins M., Lalla N. D., Omodei N., Baldini L., 2019, Nuclear Instruments and Methods in Physics Research A, 936, 224
Radhakrishnan V., Cooke D. J., 1969, Astrophys. Lett., 3, 225
Sgrò C., 2017, in Society of Photo-Optical Instrumentation Engineers (SPIE) Conference Series. p. 103970F, doi:10.1117/12.2273922
Weisskopf M. C., et al., 2016, in den Herder J.-W. A., Takahashi T., Bautz M., eds, Society of Photo-Optical Instrumentation Engineers (SPIE) Conference Series Vol. 9905, Space Telescopes and Instrumentation 2016: Ultraviolet to Gamma Ray. p. 990517, doi:10.1117/12.2235240
Weisskopf M. C., et al., 2021, arXiv e-prints, p. arXiv:2112.01269
Wolff M. T., et al., 2016, ApJ, 831, 194

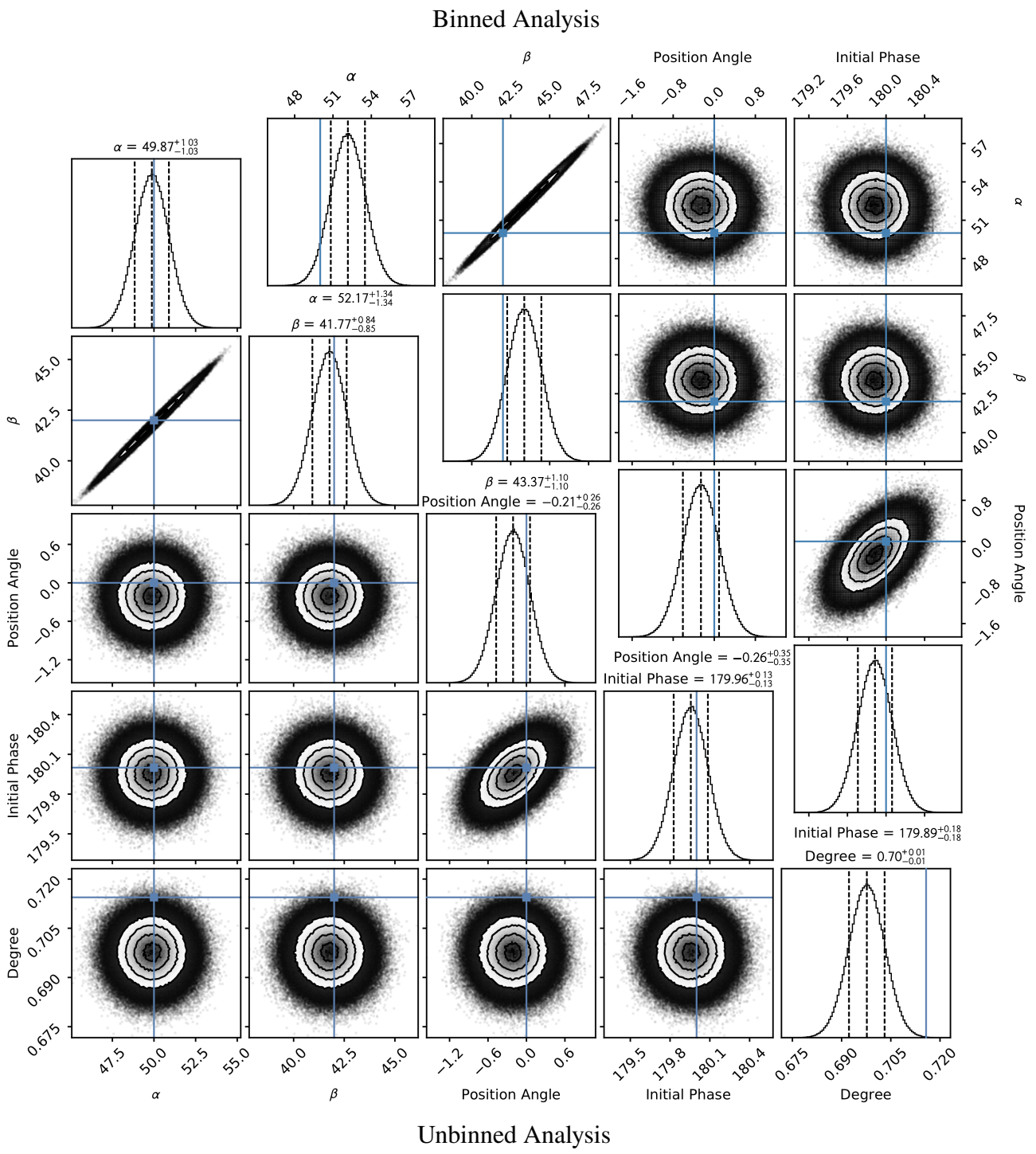

Figure 3. Results of a fit to a single realization of the Her X-1 Observation using the RVM model. The contours depict the uncertainty distribution for a single fit. The blue lines show the true values of the model.

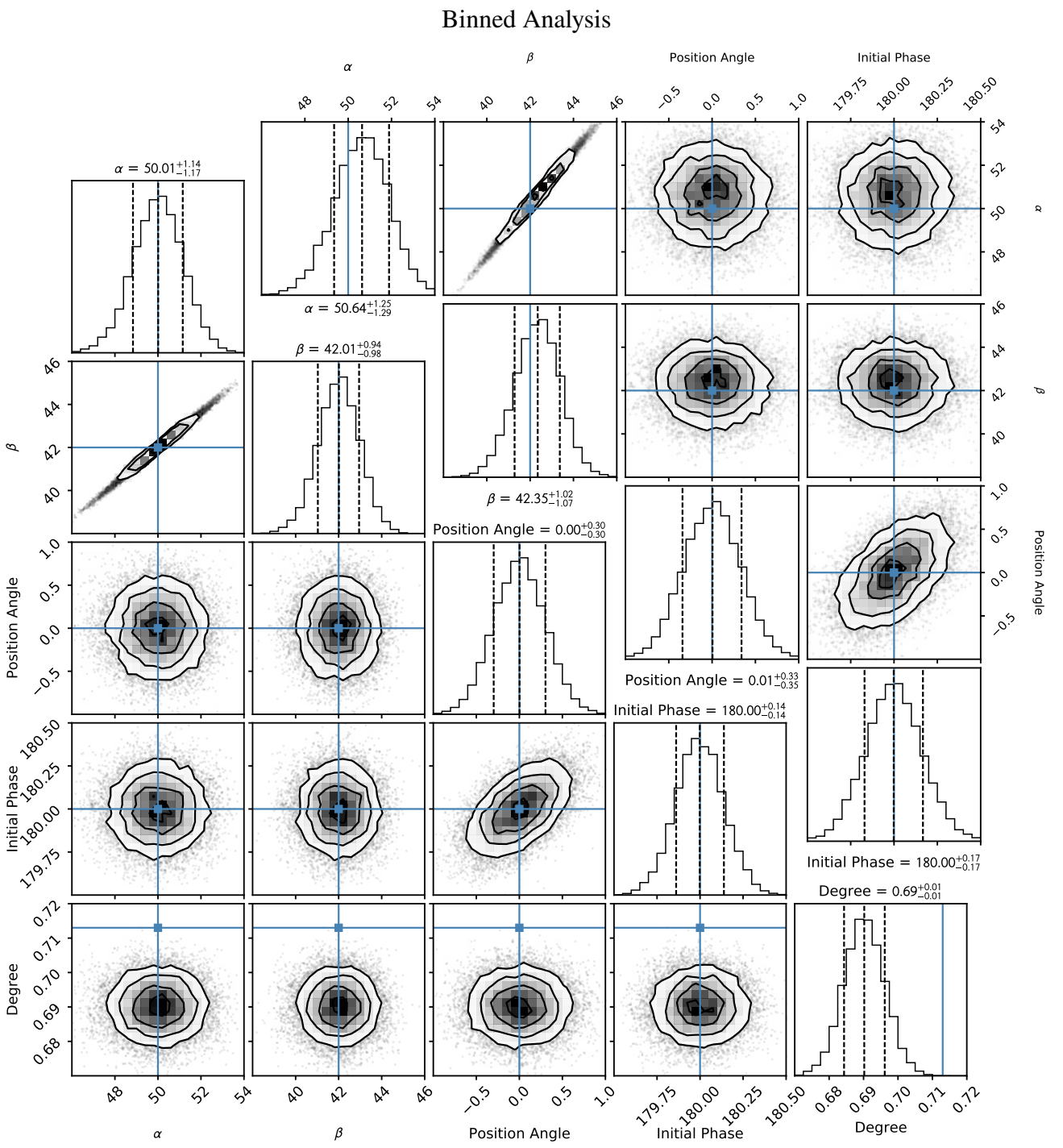

Figure 4. Results of the fit of 12, 700 realizations of the Her X-1 observation using the RVM model. Notice that the unbinned analysis yields an unbiased estimator for the angles α and β while the binned approach yields a systematic bias at the one-half-sigma level. The unbinned likelihood function (without energy redistribution) underestimate the mean polarization degree.

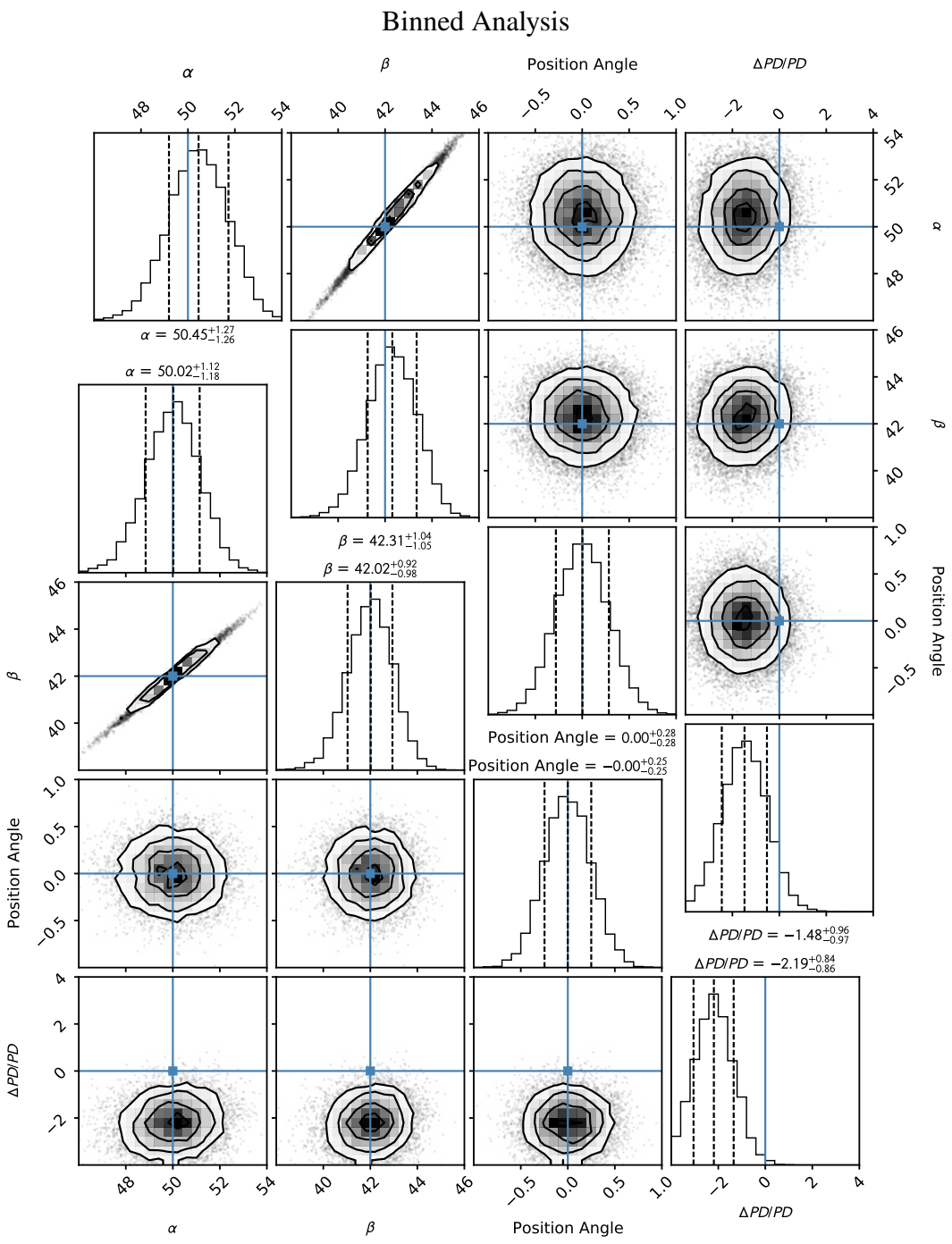

Figure 5. Results of the fit of 7,400 realizations of the Her X-1 Observation using the underlying Caiazzo & Heyl (2021b) model. Again the unbinned analysis yields an unbiased estimator for the angles α and β while the binned approach yields a systematic bias at the one-half-sigma level. Both techniques underestimate the polarization of the object: they are a biased estimator for the polarization degree, $\Delta PD/PD\,[\%]$

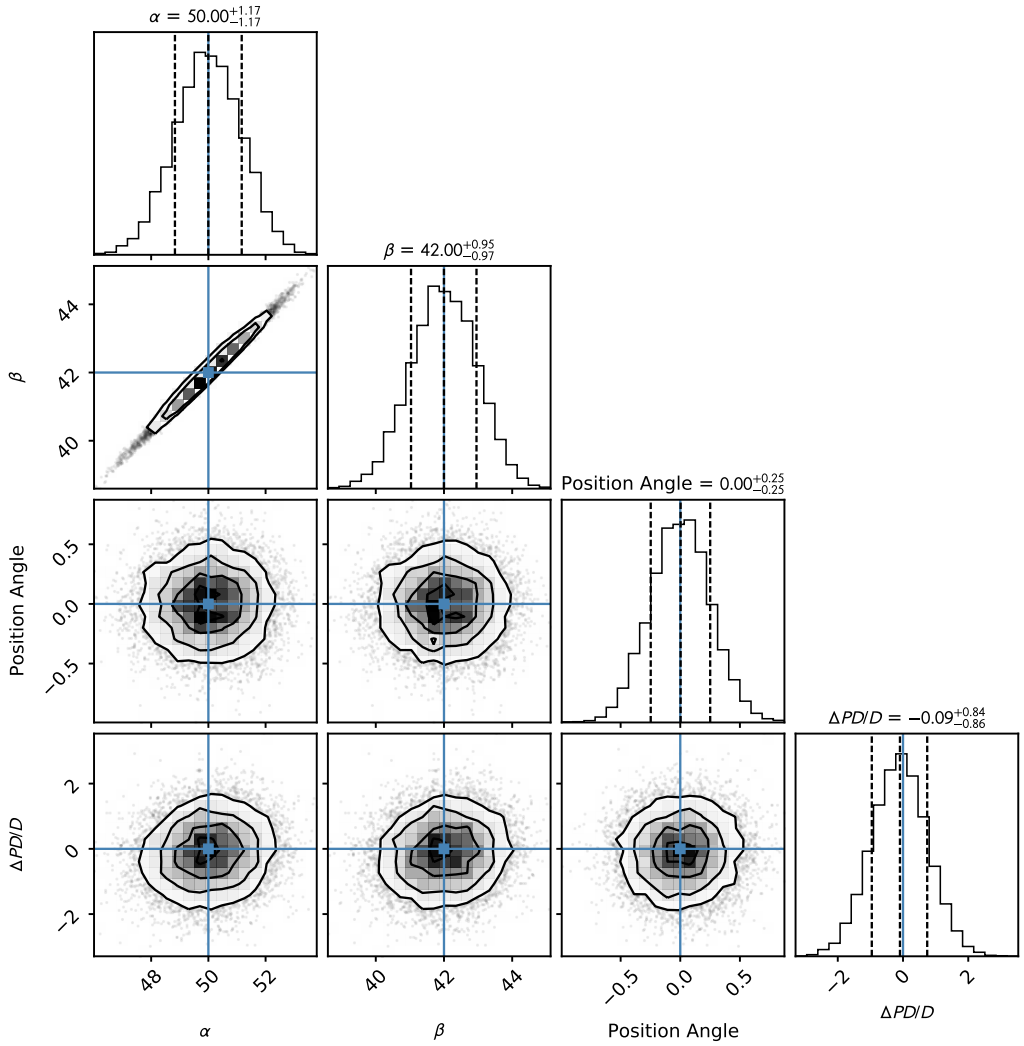

Figure 6. Results of the fit of 9,400 realizations of the Her X-1 Observation using the underlying Caiazzo & Heyl (2021b) model including energy redistribution. All of the values are now unbiased with typically uncertainties of one percent including $\Delta PD/PD\,[\%]$.

```python
def angRVM(alpha,beta,phase):
    tanhalfC,halfamb,halfapb=np.tan(phase*np.pi),np.radians(alpha-beta)/2,np.radians(alpha+beta)/2
    return (np.arctan2(np.sin(halfamb),np.sin(halfapb)*tanhalfC)-
            np.arctan2(np.cos(halfamb),np.cos(halfapb)*tanhalfC))

def likelihoodRVM(param):
    ang=angRVM(param[1],param[2],phasedu-param[4])+np.radians(param[3])
    return(-np.sum(np.log(1+0.5*modfdu*param[0]*(np.cos(2*ang)*qdu+np.sin(2*ang)*udu))))

def likelihoodModel(alpha,beta,deltadeg):
    # calculate model for parameters
    model.reset_geometry(alpha,beta)

    logL=0
    npred=0
    # looping over IXPE detectors
    for rmf, arf, mdf, qdu, udu, phasedu, phadu in
        zip(rmflist, arflist, modflist, qdulist, udulist, phasedulist, phadulist):

        flux_conv=np.dot(rmf,np.transpose(arf(effae)*np.transpose(model.flux)))

        # average over phase and sum over channels
        npred+=np.sum(np.mean(flux_conv,axis=-1))*exptime

        u_norm=np.dot(rmf, np.transpose(arf(effae)*mdf(effae)*np.transpose(model.u_data)))/flux_conv
        q_norm=np.dot(rmf, np.transpose(arf(effae)*mdf(effae)*np.transpose(model.q_data)))/flux_conv

        u_spline = xInterpolatedBivariateSpline(pha_list, model.phase, u_norm,kx=3, ky=3)
        q_spline = xInterpolatedBivariateSpline(pha_list, model.phase, q_norm,kx=3, ky=3)

        # calculate U/I and Q/I for the model for each photon from this DU
        um=u_spline(phadu,phasedu)
        qm=q_spline(phadu,phasedu)

        # sum over photons from this DU
        logL+=np.sum(np.log(1+0.5*(1+deltadeg)*(qdu*qm+udu*um)))
    return logL-npred
```

Figure A1. Python Code for RVM Model and General Model including Energy Redistribution.

APPENDIX A: SAMPLE CODE FOR LIKELIHOOD CALCULATIONS

A code snippet of the unbinned technique including the energy dispersion is shown in Figure A1. The likelihood function for the underlying model is defined in the function `likelihoodModel`. The main `Python 'for'` loop iterates over the 3 detector units of *IXPE*. The instruments response functions `rmf`, `arf`, and `mdf` correspond to the energy dispersion (loaded as a matrix), effective area (loaded as a function), and the modulation factor (loaded as a function), respectively, which are obtained from IXPEObsSim. The event information `qdu`, `udu`, `phasedu`, `phadu` correspond to the Stokes q and u, phase, and event pulse height, respectively. The `'model'` class loads the Her X-1 model for the flux and Stokes Q and U, which are energy- and phase-dependent, as well as geometry-dependent on the α and β angles. The convolved models $\langle \mu_u Q_m \rangle$ and $\langle \mu_u U_m \rangle$ are computed in `qm` and `um`.

This paper has been typeset from a TEX/LATEX file prepared by the author.